

## Soil Water Dynamics in the Root Zone of a Micro-Sprinkler Irrigated Almond Tree

Kouman S. Koumanov<sup>1</sup>, Jan W. Hopmans<sup>2</sup>, and Larry W. Schwankl<sup>2</sup>

<sup>1</sup> Fruit Growing Institute, Plovdiv, Bulgaria

<sup>2</sup> Dept of LAWR, University of California, Davis, U.S.A.

**Keywords:** root water uptake, microsprinkling, water balance, fruit trees

### Abstract

The spatial and temporal pattern of root water uptake in partially wetted soil was studied in the root zone of a six-year old micro-sprinkler irrigated almond tree. The water balance of about one quarter of the root zone's wetted soil volume (2.0 x 2.0 x 0.9 m) was determined by neutron probe and tensiometer measurements. Soil water content was measured at depths of 15, 30, 45, 60, 75, and 90 cm using PVC neutron probe access tubes, installed in a square grid of 50cm spacing to a depth of 120cm. Soil water potential gradients at the bottom of the monitored soil volume were estimated by eight pairs of tensiometers at depths of 82.5 and 97.5 cm, installed in a regular pattern between the access tubes. After linear interpolation of the tensiometer data across the experimental plot, vertical water fluxes at the 90 cm soil depth were evaluated for all access tubes locations. Neutron probe and tensiometer readings were taken at time intervals of 4 to 24 hours. The rate of soil water depletion was calculated and used to estimate the spatial and temporal distributions of root water uptake. Soil water dynamics was studied in two stages: 1) during a week of conventional irrigation management with three irrigation events; and 2) during a period of 16 days without irrigation, after the monitored soil volume was thoroughly moistened so that soil water was easily available everywhere, initially. The zones of maximum root water uptake were the same for both stages in periods of high local rates of water application. Hence, the almond tree appeared capable to redirect its root activity towards regions of the most favorable water regime with minimum soil water stress. After water applications, root water uptake developed initially near the tree trunk, progressing towards the periphery of the root system, shifting to root zone regions with minimum soil water stress, thereby changing locations of maximum root water uptake.

### INTRODUCTION

Proper water and soil management in orchards is essential for both sustainable agriculture and integrated food production. In general, irrigation scheduling is based on the water balance method, however, using localized irrigation, it is difficult to evaluate most of water balance terms. An additional complication arises from the non-uniformity of water uptake within the root zone, as roots develop preferentially in the wetted soil volume (Sakovich and Post, 1986; Bielorai, 1985) to compensate for root suberization and relative root inactivity in the non-wetted soil (Kramer and Boyer, 1995, p.146). Suberized roots need several days to regain their activity after soil wetting (Kramer, 1950), so that the rainfall term of the water balance may only apply to a fraction of the root zone. Therefore, efficient water management in micro-irrigated rooting systems

depends on knowledge of the spatial and temporal distribution of root water uptake, as well as on the ability to predict variations of soil water status in the root zone after irrigation. Whereas much is known about the root morphology of trees, including the spatial distribution of roots under localized water application, information to date on the spatial and temporal distribution of root water and nutrient uptake is limited, especially for partial-wetted soils (Clothier, 1989; Kramer and Boyer, 1995; Ben-Asher, 2000). Root water uptake models that can describe spatial and temporal patterns were developed by Coelho and Or (2000) and Vrugt et al (2001).

To provide experimental data for the development, verification and calibration of root water uptake models, thereby improving microirrigation scheduling and management, a field study was initiated in a micro-sprinkler irrigated almond orchard. This study was part of a larger project for evaluation of the physical performance of various microirrigation systems in orchards (Schwankl et al., 1996). The objective of the present study is to analyze the spatial and temporal root water uptake patterns of a micro-sprinkler irrigated almond tree. The daily water balance, water application uniformity and application efficiency of this micro-sprinkler system were discussed in a previous paper by Koumanov et al. (1997).

## **MATERIALS AND METHODS**

The investigation was conducted during the summer of 1995 in a six-year old almond orchard (Nickels Ranch), located 90 km north of Davis, California, in the Sacramento Valley. The almond trees (*Prunus amigdalus*) in the experimental plot were of the 'Butte' cultivar, grafted on 'Lovel Peach' rootstock. Tree spacing was 4.8 x 6.6 m and the canopy coverage of the soil surface was 60%. The majority of soils in the orchard were classified as the Arbuckle series with young alluvial deposits of at least 0.60 m, overlaying an old clay deposit within 1.50 m from the soil surface, Table 1. Additional information on the soil data are presented in Koumanov et al. (1997).

Micro-sprinkler irrigation was applied on about one third of a 8.8 ha almond orchard. The micro-sprinklers (Bowsmith Fan-jet<sup>1</sup>) were of the fixed head type, producing 22 single streams of water in a full circle wetting pattern. At an operating pressure of 0.15 MPa, the micro-sprinkler average discharge was about 41.7 L h<sup>-1</sup> over an effective wetting radius of approximately 2.0 m.

The study objectives were addressed using detailed soil water monitoring in the root zone of a single representative almond tree. The experimental plot covered about one quarter of the wetted area of one micro-sprinkler (Fig.1). In the 2.0 x 2.0 m monitored area, 25 PVC neutron probe access tubes (diameter 50 mm) were installed in a square grid using a separation distance of 50 cm, to a depth of 1.2 m. In addition, eight pairs of tensiometers were installed in a regular pattern between the access tubes at depths of 82.5 cm and 97.5 cm, respectively. Since the water application rates were low and no water ponding occurred, there was no evidence of the instruments affecting the soil water regime, despite that a large number of neutron probe access and tensiometer tubes were concentrated in a relatively small area. After linear interpolation of the tensiometer data, vertical water fluxes across the lower boundary (90 cm depth) were evaluated for all neutron probe access tube locations through Darcy's equation, using parameter values reported by Andreu et al. (1997).

---

<sup>1</sup> Bowsmith, P.O.Box 428, Exeter, CA 93221, USA.

The soil water dynamics was studied for two irrigation periods. In the first period (8/18–8/25/95), the experimental plot was irrigated three times (8/18, 8/21, and 8/23). The corresponding applied water amounts to the 2.25 x 2.25 m experimental area were 125 L (24.7 mm), 85 L (16.8 mm), and 106 L (20.9 mm). Irrigation scheduling was based on California Irrigation Management Information System (CIMIS) data. Additional information on the applied irrigation scheduling can be found in Koumanov et al. (1997). Neutron probe and tensiometer readings were collected before and after each water application, and daily at about 6:00, 10:00, 14:00, and 18:00 hours. In addition, readings were taken nightly after the 8/18 irrigation – at 22:00 and 2:00 o'clock. During the second period (9/13–9/29), soil water depletion was monitored during a 16-day period with no irrigation. On 9/13, the micro-sprinkler system was used to wet up the entire 90 cm soil profile above field capacity, after which the irrigation was cut off. Neutron probe and tensiometer readings were taken immediately after water applications at 13:00, 15:00, and 18:00 hours, every four hours daily (at 6:00, 10:00, 14:00, and 18:00 o'clock) from 9/14 – 9/17, and only one time daily at about 10:00 o'clock from 9/18 – 9/29.

In both experimental periods, the water balance was computed between each time interval. Root water uptake can be estimated easily from the water content measurements only, if water fluxes (drainage and/or evaporation, and between layers) can be considered insignificant. It will be shown, based on experimental results, that this is the case for the four-hour time intervals between measurements applied in the present study. The soil water content and soil water depletion rates were evaluated for the 0–22.5, 22.5–37.5, 37.5–52.5, 52.5–67.5, 67.5–82.5, and 82.5–97.5 cm soil depth intervals, corresponding to the 15, 30, 45, 60, 75, and 90 cm depth measurements with the neutron probe. Soil water content changes were considered insignificant, if the water content changes as measured between two consecutive measurement times were smaller than the precision of the neutron probe. This precision, as determined from repeated neutron probe measurements was  $0.003 \text{ m}^3 \text{ em}^{-3}$ , which was about equal to its values provided by the manufacturer.

## RESULTS AND DISCUSSION

### First Experimental Period

Most of the variations in soil water content occurred in the upper 22.5 cm soil layer only, as measured by the 15-cm depth neutron probe readings. We believe that the micro-irrigation scheduling method that was based on drip-irrigation resulted in under-irrigation and inadequate wetting of the soil profile. Consequently, most of the tree root activity was also concentrated in the surface soil layer. For the remaining larger part of the monitored soil volume, measured soil water content fluctuations were smaller than the precision of the neutron probe. Dry soil and small soil water matric potential gradients resulted in very low values of vertical water flux across the lower boundary. Between water applications, water flow was generally directed upwards (capillary rise), with maximum flux values occasionally at about  $0.0002 \text{ cm h}^{-1}$ . We estimated the evaporation  $E$  ( $\text{mm day}^{-1}$ ) from bare soil after removing the cover of the experimental plot for field capacity determination (Cassel and Nielsen, 1986). From the estimated evaporation values we calculated the rates of soil water depletion  $R$  ( $\text{cm}^3 \text{ cm}^{-3} \text{ h}^{-1}$ ) for each of the two surface layers. Except for the very first measurement immediately after uncovering of the soil surface, all values for  $R$  were less than  $0.0005 \text{ cm}^3 \text{ cm}^{-3} \text{ h}^{-1}$ . Hence, the change of soil water content in the top layer for the four-hour time intervals between measurements did not exceed  $0.002 \text{ cm}^3 \text{ cm}^{-3}$ , which was less than the precision of the neutron probe. In

other words, the influence of evaporation on soil water depletion could be assumed insignificant compared to root water uptake when considering the four-hour time intervals between measurements.

According to the results obtained, the almond tree appeared capable to redirect its root activity towards the zones of the most favorable water regime. The temporal changes in irrigation water application pattern of the sprinkling system had a beneficial effect on the shallow root system, maintaining an active root system over a large part of the experimental plot. However, the time series of water content measurements did not show soil water depletion by root uptake in zones of high water content at the 60-75 cm depth, likely because of the absence of active tree roots at the larger soil depths. Also, soil surface water storage did not change much at the larger radial distances from the tree (Fig. 2). Apparently, the active almond tree roots developed preferentially close to the trunk provided there is sufficient water to meet plant water requirements. Similar results were obtained for drip irrigated peach trees grown in lysimeters (Koumanov et al., 1998; Stoilov et al., 1999).

The rate and the spatial distribution of root water uptake varied significantly, depending on soil water availability, the distance from the tree trunk, and the intensity of meteorological factors during the day. As an example, Fig. 3 presents the spatial variation of surface soil water depletion rate ( $\text{m}^3 \text{m}^{-3} \text{hr}^{-1}$ ) on 8/19, the day after the first water application at 10:00, 14:00, and 18:00 o'clock, respectively. The initial locations of maximum water depletion rates by root water uptake were close to the tree (bottom left corner in Fig. 3a). Later, as evidenced by the water depletion maps in Figs. 7b and c, the zones of maximum water uptake moved away from the tree trunk, with roots exploring the wetter soil regions. During the periods between water applications, the pattern of soil water depletion resembled concentric circles with the tree trunk at the center and a radius about equal to the vertical projection of the tree crown. As expected, no soil water depletion or root activity was measured in the experimental plot during night periods.

## **Second Experimental Period**

During the second experimental period, the soil water status was monitored after fully wetting the root zone. For the majority of points, except for a few at the periphery of the grid, the soil profile was wetted above FC. The rates of drainage below root zone were mostly smaller than 0.003 cm/h or 0.7 mm/d. We assume that the low drainage rates have not affected the root water uptake patterns that developed mostly in the upper 20–25 cm soil layer. Likely, the insufficient soil wetting below the 25 cm soil depth during the irrigation season has resulted in root suberization and reduced development of active roots.

As demonstrated in Fig. 4, root water uptake developed initially (9/14) close to the tree trunk, shifting to wetter parts of the root zone as water becomes depleted there. Also Green et al. (1997) and Andreu et al. (1997) have reported on temporal changes of maximum root water uptake patterns, as determined by variations in water availability.

Throughout the first few days of the second experimental period, the daily maximum values of water uptake rates occurred between 10:00 and 18:00 o'clock and negligible uptake was observed during the night. In the lateral direction, the pattern of soil water depletion decrease radially outwards from the tree trunk, with the radial distance controlled by the vertical projection of the tree crown. In the vertical direction, water depletion started at the soil surface and progressed downwards with time. However, daily maximum root uptakes decreased with time as caused by the reduced water content in the

upper soil layers with the active roots, and the absence of roots in the lower soil layers despite that water content was relatively high there. The maximum values of total soil water depletion were found at the soil surface. Evaporation rates were not measured, though there is no evidence that it would affect the spatial root water uptake patterns. The lesser role of evaporation was also confirmed by the low rates of soil water depletion in surface soil zones with low root activity.

Root water uptake rate depends on root density; however, fluxes into the roots are directly controlled by the gradient in water potential between the roots and the surrounding soil. In the range of soil water potential where the root resistance is the limiting factor controlling water uptake, maximum water uptake will occur in the zones of maximum soil water potential or water content (Veihmeyer and Hendrickson, 1938; Hough et al., 1965). Following this same reasoning, it is expected that the tree root water potential increases with increasing distance of the root from the tree trunk, thereby causing a radial spatial root water uptake distribution. Hence, we postulate that in a uniformly-wetted soil, root extraction will be higher near the trunk, because of the larger water potential gradient there. In summary then, the spatial distribution of root water uptake  $S(x, y, z)$  may be expressed as a function of root density ( $d$ ), soil water potential, ( $h_s$ ) and root water potential ( $h_r$ ), i.e.  $S(x, y, z) = f(d, h_s, h_r)$ , where  $h_r = f(\lambda)$ , with  $\lambda$  denoting the distance from the tree trunk.

Although the experimental results are solely for a single almond tree, it is expected that the established pattern of root water uptake are likely for most other micro-sprinkler irrigated fruit tree species.

## CONCLUSIONS

Despite that water application was nonuniform, soil moisture uniformity prior to irrigation was large, and was caused by differential root water uptake in the surface soil. Throughout the experiments, the roots of the almond tree were capable to redirect their areas of maximum root activity towards the zones of the most favorable water regime, thereby resulting in fairly uniform water content distributions.

Typically, zones of maximum root water uptake developed from the tree trunk towards the outer regions of the root zone, shifting to wetter parts of the root zone domain. Consequently, soil water depletion patterns formed a radial pattern around the tree trunk. There was little root development below the soil surface layer and soil water depletion was small even if the total 90-cm soil profile was wetted. Thus, in summary, factors controlling root water uptake in irrigated tree crops are (1) spatial distribution of active roots, (2) root zone water contention distribution, and (3) distance from the tree trunk. We believe that our results show that water use efficiency could be increased if irrigation water was applied in a circular pattern with decreasing water application with increasing distance of the tree trunk. Such a surface water application pattern can be achieved by a pair of sector-operating microsprinklers (e.g. 210° each), located at both sides of the tree trunk.

## ACKNOWLEDGEMENTS

This research was supported in part by Grant IS-2131-92RC from the U.S.-Israel Binational Agricultural Research and Development fund (BARD). We also thank the International Atomic Energy Agency (IAEA) for the funding for Dr. Koumanov's fellowship in the Department of Land, Air and Water Resources at the University of California, Davis for the June 1995 – March 1996 period.

### Literature cited

- Andreu, L., Hopmans, J.W. and Schwankl, L.J., 1997. Spatial and temporal distribution of soil water balance for a drip-irrigated almond tree. *Agricultural Water Management* 35: 123-146.
- Bielorai, H., 1985. Moisture, salinity and root distribution of drip irrigated grapefruit. *Proc. 3<sup>rd</sup> Int. Drip/Trickle Irrigation Congr., Fresno, Vol 2: 562-567.*
- Cassel, D.K. and Nielsen D.R., 1986. Field capacity and available water capacity. In: Klute, A. (Ed.), *Methods of Soil Analysis, Part 1 Physical and Mineralogical Methods. SSSA Book Series: 5*, pp. 901-924.
- Clothier, B.E., 1989. Research imperatives for irrigation science. *Journa of Irrigation and Drainage Engineering* 115(3): 421-448.
- Coelho, F.E. and D. Or. (1996). A Parametric model for two-dimensional water uptake intensity by corn roots under drip irrigation. *Soil. Sci. Soc Am. J.* **60**, 1039-1049.
- Green, S.R., Clothier, B.E. and McLeod, D.J., 1996. The responce of sap flow in apple roots to localised irrigation. *Agricultural Water Management* 33(1): 63-78.
- Hough, W.A., F.W. Woods, amd M.L. McCormack, 1965. Root extension of individual trees in surface soilsof a natural longleaf pine-turkey oak stand. *For. Sci.* 11, 223-242 [cited in Kramer and Boyer, 1995].
- Koumanov, K., Dochev, D. and Stoilov, G., 1998. Investigations on fertigation of peach on three soil types - patterns of soil wetting. *Bulg. J. Agric. Sci.* 4: 745-753.
- Koumanov, K.S., Hopmans, J.W., Schwankl, L.W., Andreu, L. and Tuly, A., 1997. Application efficiency of micro-sprinkler irrigation of almond trees. *Agricultural water Management* 34: 247-263.
- Kramer, P.J. and Boyer, J.S., 1995. *Water Relations of Plants and Soils.* Academic Press, San Diego, 495 pp.
- Kramer. P.J., 1950. Effects of wilting on the subsequent intake of water by plants. *Am. J. Bot.* 37:280-284.
- Sakovich, N.J. and Post, S.E.C., 1986. Lemon root distribution in sprinkler, drip systems. *Citrograph* 71(7): 143-144.
- Schwankl, L.J., Edstrom, J.P. and Hopmans, J.W., 1996. Performance of micro-irrigation systems in almonds. *Proc. 7<sup>th</sup> Int. Conf. Water Irrigation.* Tel Aviv, Israel, May 13-16.
- Stoilov, G., K. Koumanov, and D. Dochev (1999). Investigations on fertigation of peach on three soils.I.Migration and localization of nitrogen. *Bulg. J. Agric. Sci.*, 5: 605-614.
- Veihmeyer, F.J. and A.H. Hendrickson, 1938. Soil moisture as an indication of root distribution in deciduous orchards. *Plant Physiology* 13, 169-177 [cited in Kramer and Boyer, 1995].
- Vrugt, J.A., J.W. Hopmans and J. Simunek. (2001a). Twodimensional root water uptake model for a sprinkler-irrigated almond tree. *Soil Sci. Soc. Amer. J.* **65**, 1027-1037.
- Willoughby, P. and Cockroft, B., 1974. *Proceedings, 2-nd International Drip Irrigation Congress*, pp.439-445.

## Tables

Table 1. Particle size distribution, volumetric gravel content, dry bulk density, and volumetric soil moisture at field capacity as a function of soil depth.

Depth (cm)	Soil texture (%, by weight)			Volumetric gravel content ( $\text{m}^3 \text{m}^{-3}$ )	Bulk density ( $\text{kg m}^{-3}$ )	Soil moisture at field capacity ( $\text{m}^3 \text{m}^{-3}$ )
	Sand	Silt	Clay			
15				0.25	1598	0.196
30	53.0	41.0	6.0	0.29	1610	0.185
45				0.29	1646	0.214
60	58.0	32.5	9.5	0.40	1738	0.252
75				0.31	1807	0.272
90	67.0	25.0	8.0	0.30	1790	0.229

## Figures

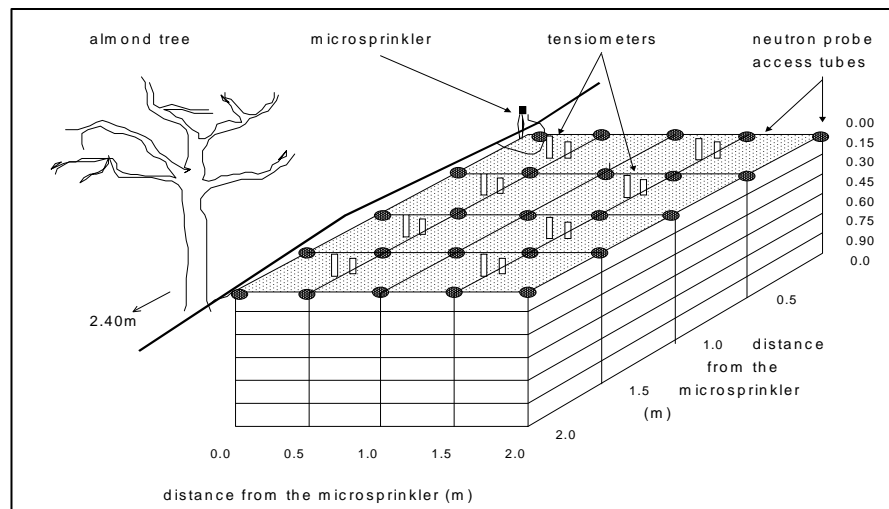


Fig. 1 Schematic presentation of the experimental plot.

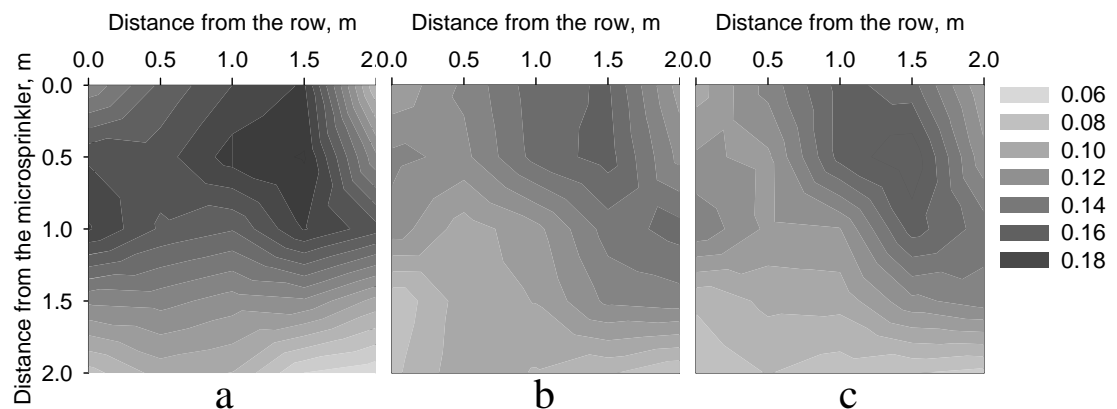


Fig. 2 Soil surface water content ( $\text{m}^3 \text{m}^{-3}$ ) distribution in the upper 22.5 cm soil layer before the water applications on 8/18, 8/21, and 8/23/95.

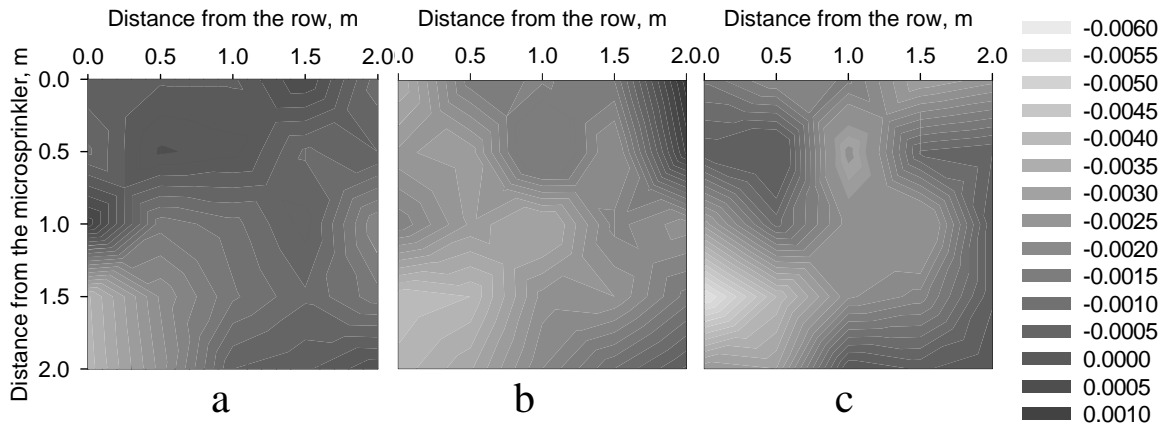


Fig. 3 Soil water depletion rate ( $\text{m}^3 \text{m}^{-3} \text{h}^{-1}$ ) in the top 22.5 cm soil layer, after the water application on 8/19/95 for the periods 6:00—10:00 (a), 10:00—14:00 (b), and 14:00—18:00 (c). Negative values indicate soil water depletion.

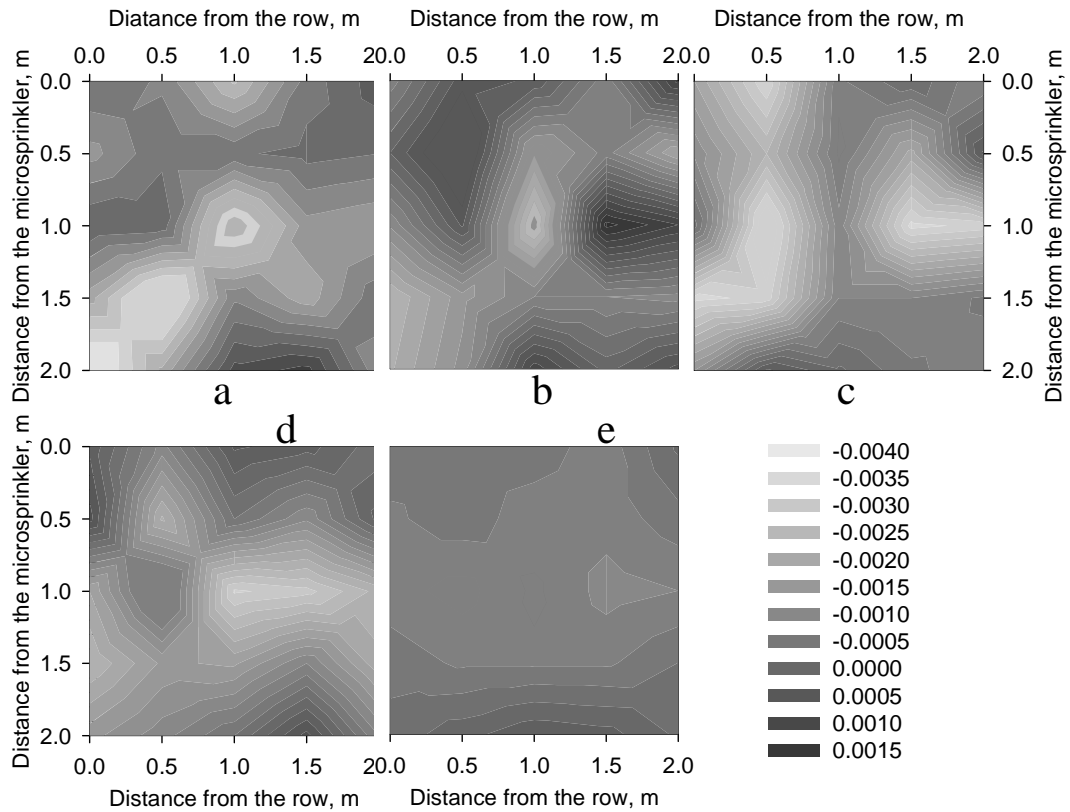


Fig. 4 Water depletion rate ( $\text{m}^3 \text{m}^{-3} \text{h}^{-1}$ ) in the upper 22.5 cm soil layer, estimated on 9/14/95 for the period 10:00—14:00 (a); on 9/15/95 for the periods 10:00—14:00 (b) and 14:00—18:00 (c); on 9/17/95 for the period 10:00—14:00 (d); and from 10:00 on 9/18 till 11:00 on 9/19/95 (e).